Supplementary Information

Nanopores with Dynamic Pore Opening Diameter

Savannah Silva,[1,#] Xavier Mleziva,[2,3,#] Anthony Dougman Cho,[1] Christopher Maffeo,[2,3] Bernadeta Srijanto,[4] Ivan V. Vlassiouk,[4] Ethan Cao,[1] Aleksei Aksimentiev,[2,3,*] Zuzanna S. Siwy[1,5,6,1*]

[1]Department of Physics and Astronomy, University of California, Irvine, Irvine, CA 92697

[2]Department of Physics, University of Illinois at Urbana–Champaign, Urbana, IL, USA

[3]Beckman Institute for Advanced Science and Technology, University of Illinois at Urbana–Champaign, Urbana, IL, USA

[4]Center for Nanophase Materials Sciences, Oak Ridge National Laboratory, Oak Ridge, TN, 37831 USA

[5]Department of Chemistry, University of California, Irvine, Irvine, CA 92697

[6]Department of Biomedical Engineering, University of California, Irvine, Irvine, CA 92697

[#] These Authors contributed equally

[1*] Corresponding Authors: aksiment@illinois.edu, zsiwy@uci.edu

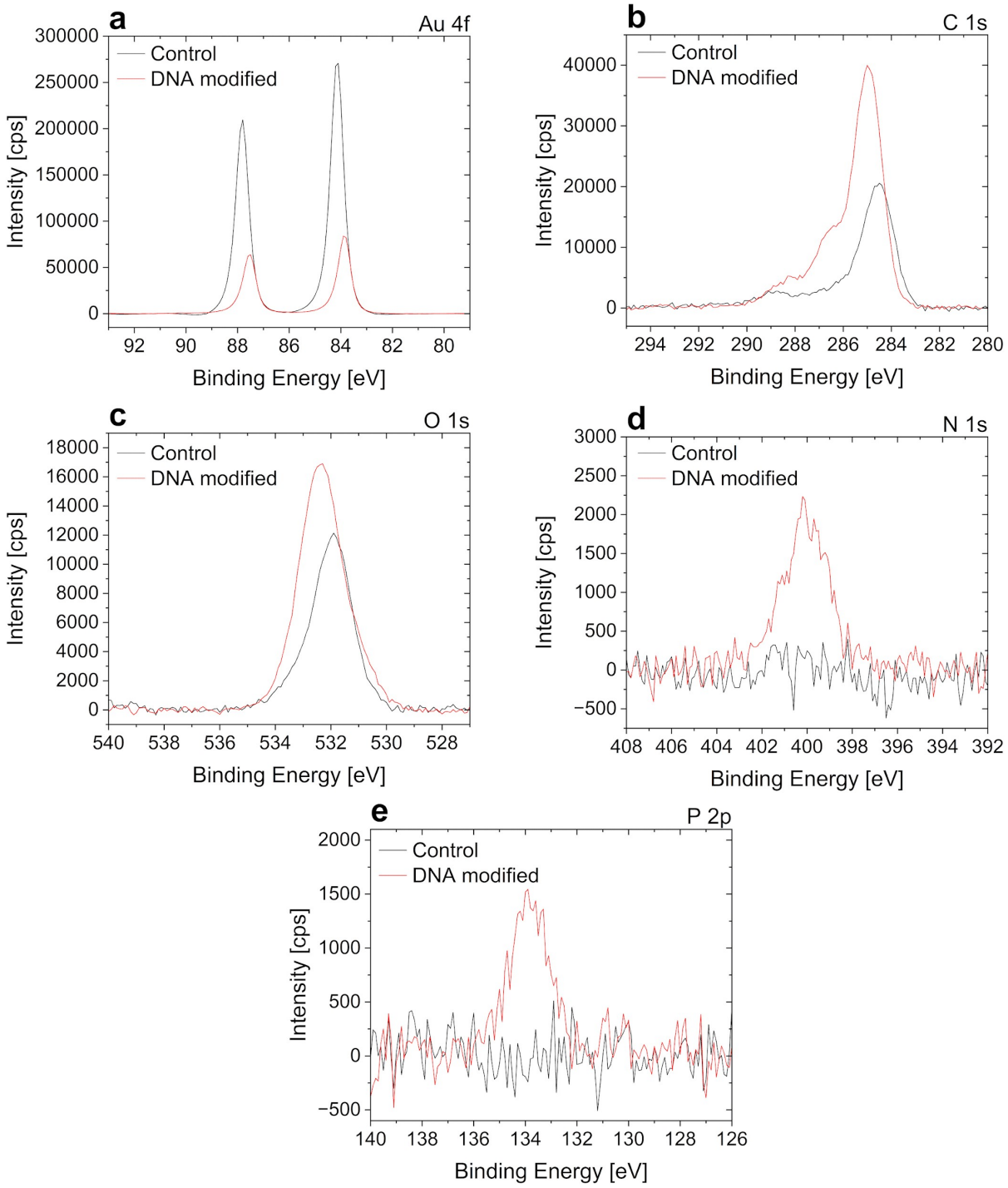

Figure S1. XPS spectra of a SiN TEM window layered with 10 nm layer of Au, modified with ssDNA (red line) and without modification (black line). (a) Au 4f, (b) C 1s, (c) O 1s, (d) N 1s, and (e) P 2p XPS spectra. The suppression of the Au 4f peak post-modification indicates the formation of the DNA layer on the Au (a). The enhancement of C 1s, O 1s, N 1s, and P 2p peaks post-modification is attributed to the sugar-phosphate backbone and nitrogenous bases of DNA and further confirms successful DNA attachment onto Au.

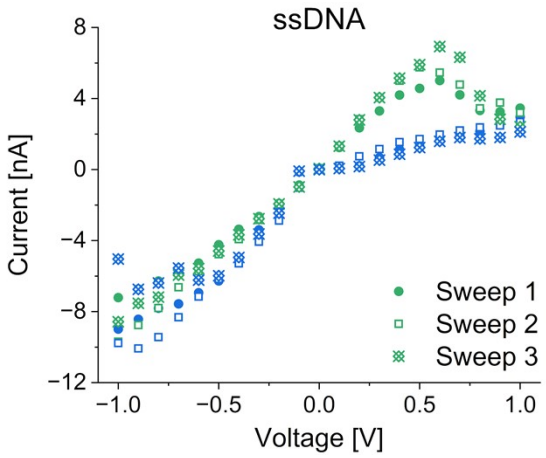

Figure S2. Raw I-V curves for an 11 nm diameter Au-SiN pore after modification with ssDNA. The raw I-V curves for three different scans in 100 mM KCl are presented for the same pore as shown in Figure 1. The different sweeps are distinguished by symbols (filled circle, empty square, cross diamond) and the forward and reverse sweeps are distinguished by color (green, blue).

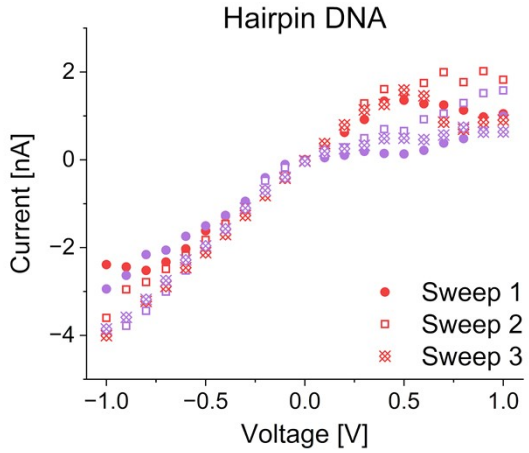

Figure S3. Raw I-V curves for a 10 nm diameter Au-SiN pore after modification with hairpin DNA. The raw I-V curves for three different scans in 10 mM KCl are presented for the same pore as shown in Figure 4. The different sweeps are distinguished by symbols (filled circle, empty square, cross diamond) and the forward and reverse sweeps are distinguished by color (red, purple).

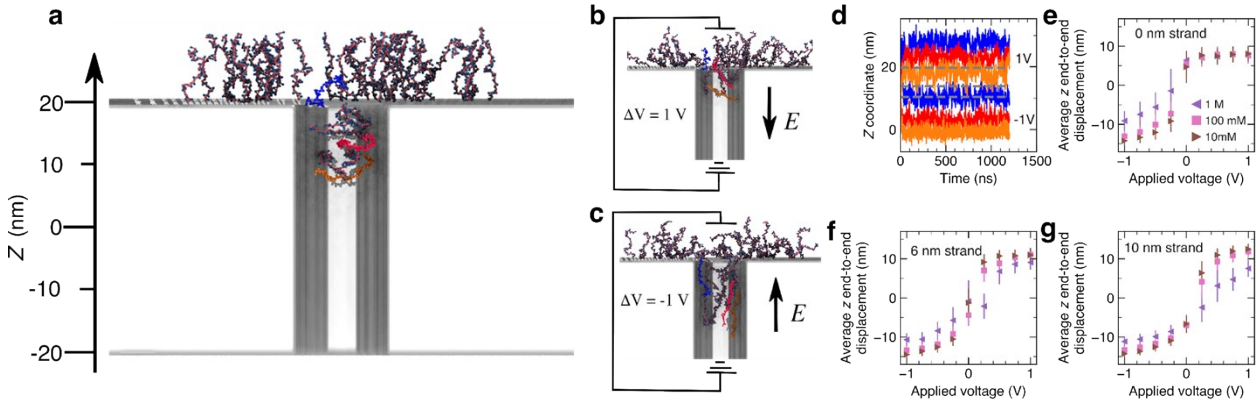

Figure S4. Asymmetric response of ssDNA conformation to polarity of the electrostatic potential. (a) Cutaway view of the simulation system containing a 15 nm diameter nanopore in a 40 nm thick membrane decorated with ssDNA. (b, c) Representative configurations of ssDNA strands in coarse-grained MD simulations carried out at +1V (b) and -1V (c) transmembrane voltage. The DNA strands highlighted in orange, red, and blue are used for quantitative analysis of ssDNA conformations. In panels a-c, non-analysis strands anchored in front of the cutaway plane at the center of the pore are not shown for clarity. (d) *Z* coordinate of the terminal nucleotide of a DNA strand attached to the nanopore surface 0 (blue), 6 (red), and 10 (orange) nm away from the membrane surface as a function of simulation time at +/- 1V. The gray lines indicate the locations of the strands' attachment within the nanopore. (e-g) Average end-to-end distance of the DNA strand attached 0, (panel e), 6 (panel f) and 10 (panel g) nm away from the nanopore entranced projected along the *z* axis. The three lines in each panel indicated data obtained at three ion concentrations. Each error bar indicates the standard deviation over a 1.2 μs trajectory.

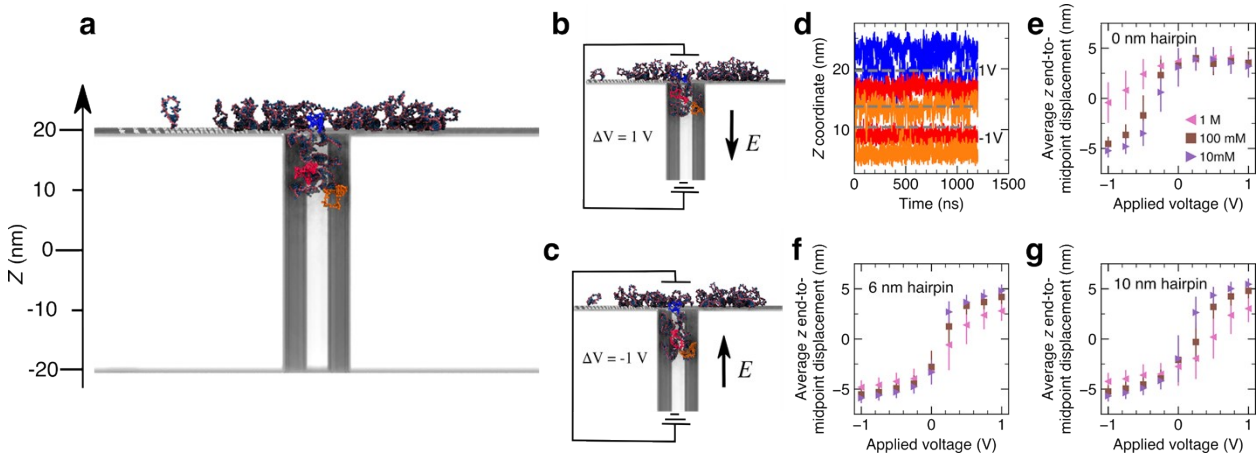

Figure S5. Response of DNA hairpins to potential gradients in a 11 nm nanopore. (a) Cutaway view of the simulation system containing an 11 nm diameter nanopore in a 40 nm thick membrane decorated with DNA hairpins. (b) Representative configurations of DNA hairpins in coarse-grained MD simulations carried out at +1V (b) and -1V (c) transmembrane voltage. The DNA hairpins highlighted in orange, red, and blue are used for quantitative analysis of DNA hairpin conformations in subsequent panels. In panels a-c, non-analysis strands anchored in front of the cutaway plane at the center of the pore are not shown for clarity. (d) *Z* coordinate of the DNA hairpin midpoint restrained at 0 (blue), 6 (red), and 10 (orange) nm away from the nanopore entrance when a bias voltage of ±1 V is applied versus the simulation time in 1 M KCl. The gray lines show the position of the restrained nucleotides of the corresponding strands along the z axis versus time. (e-g) *Z* component of the average end-to-midpoint displacement vector versus the applied bias voltage for the DNA hairpins restrained 0 (panel e), 6 (panel f) and 10 nm (panel g) away from the nanopore entrance at the specified KCl concentrations. Each error bar indicates the standard deviation over a 1.2 μs trajectory.

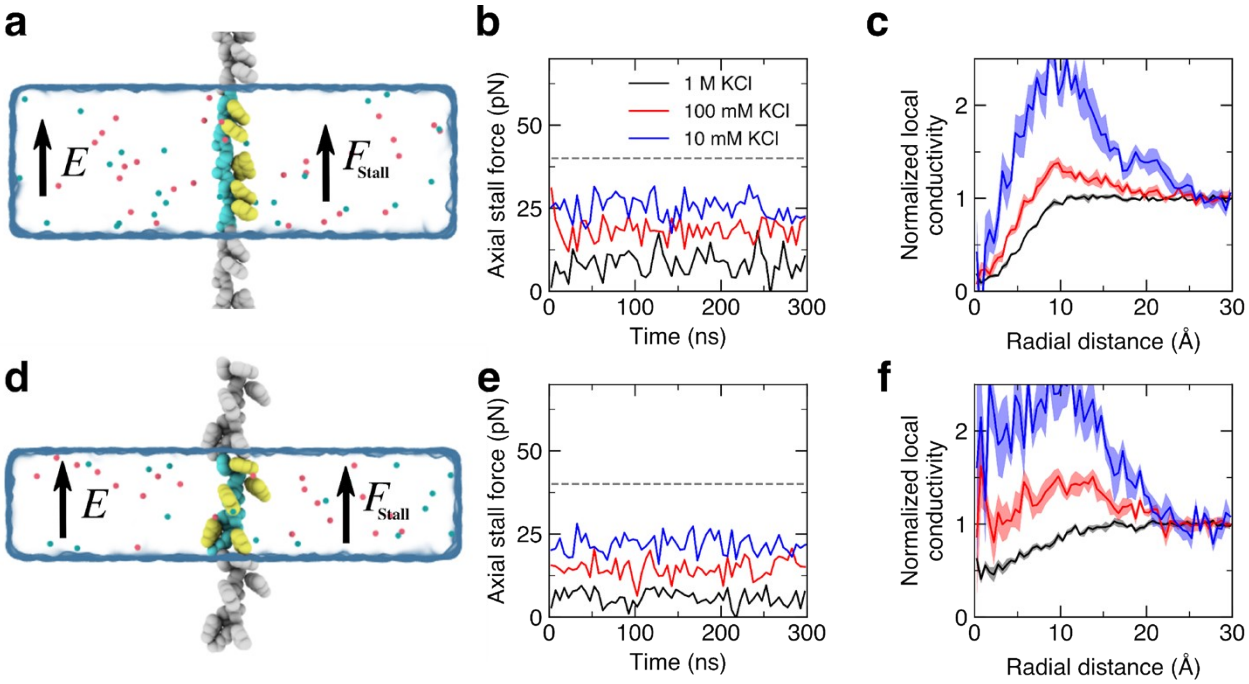

Figure S6. All-atom MD determination of the effective charge and local ionic conductivity of ssDNA. (a) Simulation system containing a five-nucleotide DNA strand connected to itself over the periodic boundary with a ~6.9 Å per nucleotide spacing solvated in 100 mM KCl electrolyte. (b) Total effective force of ssDNA under a 50 mV/nm electric field versus simulation time for the system shown in panel a. Each curve shows 5 ns block-average of a 20 ps-sampled data. The dashed line represents the total electrostatic force applied to the ssDNA (~40 pN), computed from the nominal charge of five nucleotides. (c) Local ionic conductivity as a function of radial distance from ssDNA for the system shown in panel a. The conductivity profiles were normalized by the respective bulk conductivity values. The shaded region represents the standard error of the mean from 50-ns block-averaged data. (d-f) Same as in panels a-c but for ~4.8 Å per nucleotide stretching of ssDNA.

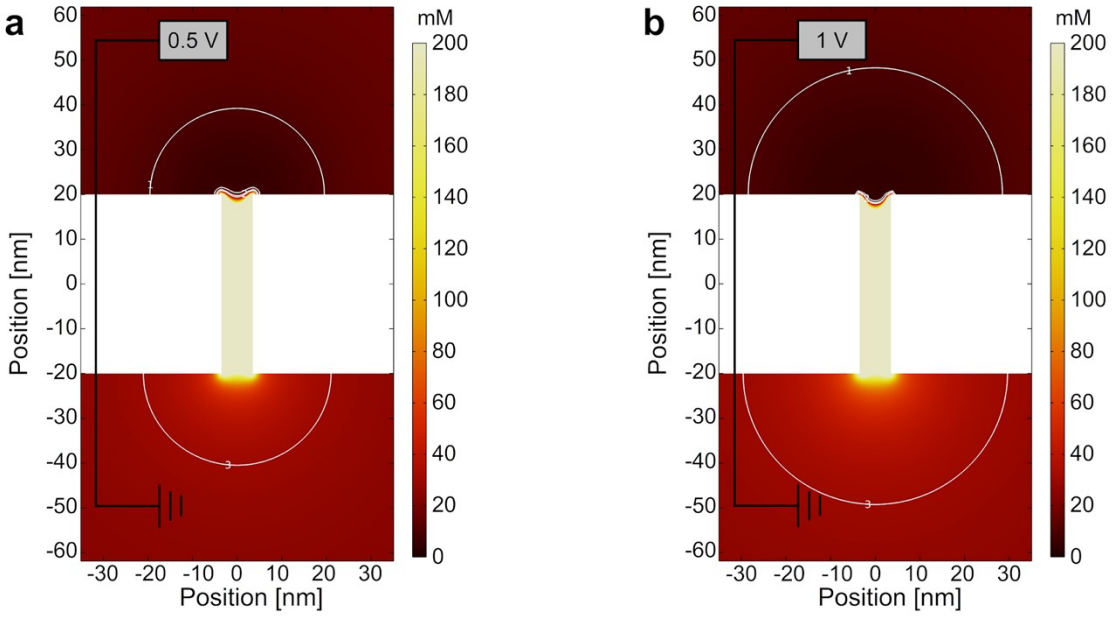

Figure S7. Simulated ion concentration profiles at a 7 nm pore opening containing a junction between two zones with different surface charges at 1 mM KCl. Cross-section heat map of local ionic concentrations presented for (a) 0.5 V and (b) 1 V applied to the working electrode. The colormap corresponds to the sum of both ions, K^+ and Cl^-, concentrations.

Movie S1: Illustrates the conformational changes of ssDNA due to a 1V transmembrane bias in a 9 nm nanopore solvated with 1 M electrolyte (Figure 5b). The video contains the first 760 ns a truncated cutaway view of coarse grained (CG) simulation. In this simulation the strands located at 0, 6, and 10 nm from the nanopore entrance utilized for end-to-end displacement vector measurement are highlighted in blue, red, and orange respectively.

Movie S2: Illustrates the conformational changes of ssDNA due to a -1V transmembrane bias in a 9 nanopore nm solvated with 1 M electrolyte (Figure 5c). The video contains the first 760 ns a truncated cutaway view of coarse grained (CG) simulation. In this simulation the strands located at 0, 6, and 10 nm from the nanopore entrance utilized for end-to-end displacement vector measurement are highlighted in blue, red, and orange respectively.

Movie S3: Illustrates the conformational changes of DNA hairpins due to a 1V transmembrane bias in an 11 nm nanopore solvated with 1 M electrolyte (Figure S3b). The video contains the first 760 ns a truncated cutaway view of coarse grained (CG) simulation. In this simulation the strands located at 0, 6, and 10 nm from the nanopore entrance utilized for end-to-midpoint displacement vector measurement are highlighted in blue, red, and orange respectively.

Movie S4: Illustrates the conformational changes of DNA hairpins due to a -1V transmembrane bias in an 11 nm nanopore solvated with 1 M electrolyte (Figure S3c). The video contains the first 760 ns a truncated cutaway view of coarse grained (CG) simulation. In this simulation the strands located at 0, 6, and 10 nm from the nanopore entrance utilized for end-to-midpoint displacement vector measurement are highlighted in blue, red, and orange respectively.

Movie S5: Illustrates the conformational changes of ssDNA due to a 1V transmembrane bias in a 15 nm nanopore solvated with 1 M electrolyte (Figure S2b). The video contains the first 760 ns a truncated cutaway view of coarse grained (CG) simulation. In this simulation the strands located at 0, 6, and 10 nm from the nanopore entrance utilized for end-to-end displacement vector measurement are highlighted in blue, red, and orange respectively.

Movie S6: Illustrates the conformational changes of ssDNA due to a -1V transmembrane bias in a 15 nm nanopore solvated with 1 M electrolyte (Figure S2c). The video contains the first 760 ns a truncated cutaway view of coarse grained (CG) simulation. In this simulation the strands located at 0, 6, and 10 nm from the nanopore entrance utilized for end-to-end displacement vector measurement are highlighted in blue, red, and orange respectively.